Mechanosensory-defective, male-sterile *unc* mutants identify a novel basal body protein required for ciliogenesis in *Drosophila*

James D. Baker, Sreedevi Adhikarakunnathu* and Maurice J. Kernan†

Department of Neurobiology and Behavior and Center for Developmental Genetics, Stony Brook University, Stony Brook, NY 11794-5230, USA

*Present address: Department of Cardiovascular and Metabolic Disease, Centocor, 145 King of Prussia Road, Radnor, PA 19087, USA
†Author for correspondence (e-mail: maurice.kernan@sunysb.edu)

Accepted 15 April 2004

Development 131, 3411-3422
Published by The Company of Biologists 2004
doi:10.1242/dev.01229

Summary

***uncoordinated* (*unc*) mutants of *Drosophila*, which lack transduction in ciliated mechanosensory neurons, do not produce motile sperm. Both sensory and spermatogenesis defects are associated with disrupted ciliary structures: mutant sensory neurons have truncated cilia, and sensory neurons and spermatids show defects in axoneme ultrastructure. *unc* encodes a novel protein with coiled-coil segments and a LisH motif, which is expressed in type I sensory neurons and in the male germline – the only ciliogenic cells in the fly. A functional UNC-GFP fusion protein specifically localizes to both basal bodies in differentiating sensory neurons. In premeiotic spermatocytes it localizes to all four centrioles in early G2, remaining associated with them through meiosis and as they become the basal bodies for the elongating spermatid flagella. UNC is thus specifically required for normal ciliogenesis. Its localization is an early marker for the centriole-basal body transition, a central but enigmatic event in eukaryotic cell differentiation.**

Key words: Cilia, Flagella, Centrioles, Mechanoreceptors, Spermatogenesis

Introduction

In many eukaryotic cells, the transition from cell proliferation to differentiation is marked by the formation of a cilium – a cellular appendage with a radially symmetric axoneme cytoskeleton, templated on a similarly symmetric basal body. It has long been known that basal bodies are identical with and derived from the centrioles that nucleate mitotic centrosomes (Meves, 1900), but the mechanisms by which a centriole is converted into a basal body remain obscure. Much work has focused on the role of centrioles and centriole-associated proteins that participate in centrosome replication and reconfiguration during the mitotic cell cycle (reviewed by Beisson and Wright, 2003; Bornens, 2002; Doxsey, 2001; Lange et al., 2000; Marshall and Rosenbaum, 2000). Less attention has been paid to the mechanisms by which a mitotic centriole is reconfigured as a ciliogenic basal body in differentiating cells. A molecular understanding of this process is nevertheless important because it may be a crucial step in the transition from cell proliferation to differentiation. Some disorders of ciliated sensory organs such as retinal photoreceptors (Liu et al., 1997; Rosenbaum et al., 1999) are the result of defective ciliary differentiation or transport. More generally, several lines of evidence now indicate that the less overtly specialized primary cilia on mammalian cells have diverse functions in developmental signaling (Pazour and Witman, 2003). For example, ciliary or basal body defects may underlie the diverse symptoms, including situs inversus, epithelial cysts, retinal dystrophy, skeletal abnormalities and obesity, that are associated with polycystic kidney disease (Pazour et al., 2000; Yoder et al., 2002) and Bardet-Biedl syndrome (Ansley et al., 2003).

Interconversion of centrioles and basal bodies occurs in eukaryotes ranging from algae to mammals. A centriole may move to the cell periphery and form a basal body in G1 of interphase, or in quiescent (G0) or differentiating cells (Rieder and Borisy, 1982; Vorobjev and Chentsov, 1982). In dividing cells, such basal bodies revert to a centriolar role prior to mitosis when the cilia are resorbed and centrosomes assemble. In many animal zygotes, the sperm flagellar basal body recruits maternal pericentriolar material to form the initial centrosome (Schatten, 1994). Centrioles are conservatively replicated once per cell cycle and segregate so that each daughter cell inherits an older and a younger centriole (Kochanski and Borisy, 1990); in mammalian somatic cells only the older centriole nucleates a cilium (Rieder and Borisy, 1982; Vorobjev and Chentsov, 1982). The older centriole is also distinguished from the younger by distal and subdistal appendages, by its ability to anchor microtubules, and by its more stable location in the cell (Piel et al., 2000). A newly assembled mammalian centriole matures over two cell cycles in a stepwise process that includes the acquisition of appendage structures and component proteins such as ninein (Piel et al., 2000), cenexin/odf2 (Lange and Gull, 1995; Nakagawa et al., 2001) and ε-tubulin (Chang et al., 2003).

By contrast, centrioles in embryos and most somatic cells of *Drosophila* are rudimentary: they are composed of microtubule doublets rather than triplets, lack most of the specialized accessory structures characteristic of mature vertebrate centrioles, and do not form primary cilia (Callaini et al., 1997;

Gonzalez et al., 1998). The only cilia in the fly are found in the peripheral nervous system (PNS) and in the male germline. In type I sensory neurons, a cilium extends from the more distal of two basal bodies at the tip of the single sensory process. This cilium is the probable site of sensory transduction, and is highly modified for this role in mechanosensory neurons. In mature spermatocytes, two pairs of centrioles with microtubule triplets migrate to the cell periphery, where their differentiated distal ends protrude from the cell (Tates, 1971) (reviewed by Fuller, 1993). During meiosis, they segregate to the meiotic spindle poles without further replication, so that a single centriole associates with each postmeiotic haploid nucleus and becomes the basal body of the spermatid flagellum. At fertilization, the entire sperm enters the acentrosomal oocyte, where the basal body recruits maternal components to form the zygotic centrosome (Callaini and Riparbelli, 1996; Callaini et al., 1999).

Thus, mutations disrupting ciliogenesis in *Drosophila* are expected specifically to affect sensory neurons and spermatids. We describe the *uncoordinated* (*unc*) gene product, which appears to be required to construct normal cilia in these cell types. Previously, *unc* mutants were found to be defective in transduction by ciliated mechanosensory neurons (Eberl et al., 2000; Kernan et al., 1994). We now show that *unc* mutant males are also defective in spermatogenesis: spermatid nuclei are detached from basal bodies and flagellar axonemes are disrupted. Axonemal defects are also found in the ciliated endings of mutant sensory neurons. *unc* encodes a large, novel, partly coiled-coil protein that is expressed specifically in ciliated sensory neurons and in male germline cells. Its localization in spermatocytes suggests an early role in reconfiguring centrioles as basal bodies.

Materials and methods

Drosophila stocks

The alleles unc^{25} through unc^{28} are described (Kernan et al., 1994). Other *unc* alleles and deletion chromosomes were obtained from the Bloomington and Umea stock centers. *unc* and *nomp* mutants were collected as pupae or pharate adults and eclosed in humid chambers. Animals were staged by collecting white pre-pupae and maintaining them at 25°C in a humid chamber. For sperm motility assays, reproductive systems from isolated 2- to 3-day-old males were dissected open in saline and examined by phase contrast and darkfield microscopy.

Immunocytochemistry

Flies containing *unc*-GFP constructs were dissected in *Drosophila* Ringers solution (Ashburner, 1989), and fixed in freshly diluted 4% formaldehyde in PBS with 0.3% Triton X-100 (PBST) for 1-2 hours at room temperature. All washes and incubations were carried out in foil-covered tubes. Tissues were rinsed three times for 1 hour in PBST and incubated overnight at 4°C in primary antibody solution containing 5% normal donkey serum. When staining with propidum iodide, 1 mg/ml RNAase A was included in the antibody solution. Anti-β-tubulin (E7), which was obtained from the Developmental Studies Hybridoma Databank, was used at 1:50; and anti-centrosomin (gift from T. Kaufman, University of Indiana, Bloomington), at 1:1000. Fluorescently labeled secondary antibodies from Molecular Probes (Alexafluor) or Jackson Laboratories (Cy5) were used at a dilution of 1:1000 in PBST with 5% normal donkey serum. Tissues were washed four times in 3 hours at 25°C, incubated with secondary antibodies overnight at 4°C, in the dark, washed four times for 1 hour, counterstained with a dilution of 10 μg/ml propidum iodide (Sigma) and mounted in 80% glycerol. Images were collected on confocal microscopes (Zeiss LSM 510 or Leica TCS SP2).

FRAP analysis

Spermatocyte cultures were established as described (Noguchi and Miller, 2003). Adult testes were isolated in Shields and Sangs medium without bicarbonate (Sigma S8398), transferred to fresh media twice and then to the culture chamber (LabtekII VWR 62407-294). Glass needles or sharpened fine forceps were used to dissect open testes and tease spermatocyte cysts onto a coverslip. Isolated cysts were selected with a Leica TCS SP2 confocal microscope and focally bleached using the time-lapse command. Centriole-bound UNC-GFP was bleached with a 15 second pulse on 100% power, sufficient to eliminate most, or all, of the signal associated with a single centriole. The centriole was monitored for 30 minutes to 1 hour by collecting *z*-series spanning the centriole pair at 1-5 minute intervals.

Electron microscopy

Testes from 2-day-old males and heads and legs from pharate adults were fixed in 2% glutaraldehyde and 2% formaldehyde in 0.1 M sodium cacodylate, pH 7.4 for 1-2 hours on ice and postfixed in 2% OsO_4 for 4 hours on ice. Tissues were dehydrated through an ethanol series, incubated in two changes of propylene oxide, and then embedded in Spurr's resin (Polysciences). Thin sections were post-stained with uranyl acetate and lead citrate before viewing with a JEM-1200EX electron microscope (80 kV).

Electrophysiology

Transepithelial and mechanoreceptor potentials were recorded as described (Kernan et al., 1994). Sound-evoked potentials were recorded from the antennal nerve as described (Eberl et al., 2000).

Molecular biology

X-ray breakpoints were mapped by field inversion gel electrophoresis and Southern blot hybridization. Cycle sequencing was performed using the ABI Big Dye cycle sequencing kit. *unc* gene fragments were amplified for sequencing from single male flies (Gloor and Engels, 1992). The cDNA LP08350 was obtained from the Berkeley Drosophila Genome Project. Genomic sequence was derived from fragments subcloned or amplified from whole P1 clones.

The 5′ end of the cDNA was extended using an RNA ligase-based RACE protocol (Chen, 1996). Total adult RNA was used as a template for first-strand cDNA using primers ATCCTGCTCCTCAATCT-GATCC and GGAACTTCACCTCGAACTCCTG from the 5′ end of the LP08350 cDNA. The adapter primer was ligated to the 5′ end using RNA ligase and a complementary primer was used in combination with the internal primer to amplify the 5′ end. Products from a second round of RACE, using 5′ primers CGCTCCTGCTTA-ATCTGCTC and GCTTCGCCCTGAACGATAAC were cloned using the Topo™ TA cloning kit (Invitrogen).

To construct a P{unc^{+}} transformation vector, the cDNA LP08350 was digested with *Sfi*I and *Xho*I and ligated in frame to a 4.65 kb *Sfi*I fragment which spanned from the beginning of the third exon of the divergently transcribed CG15445 to the third exon of *unc*. The free *Sfi*I end was blunted with T4 DNA polymerase and ligated into pCasper4 digested with *Xho*I/*Hpa*I. This and other transformation constructs were injected into embryos as described (Rubin and Spradling, 1982).

To construct the P{unc-GFP} fusion, PCR was used to modify the 5′ end of EGFP (Clontech, Palo Alto, CA) by replacing the start codon ATG with a sequence encoding the amino acids GGSRGG and including an *Xba*I site. After sequencing, the modified EGFP was cloned into a *Xba*I site at the C terminus of the predicted full-length *unc* protein. This product was cloned into the original rescue construct.

For in situ hybridization, digoxigenin-labeled sense and antisense

probes were generated by unidirectional PCR. Whole testes were probed in a protocol based on embryo in situ hybridization (Tautz and Pfeifle, 1989).

Results

Ciliary defects in *unc* mutant spermatids and sensory neurons

Cilia in *Drosophila* are restricted to type I sensory neurons, developing spermatids and sperm. *Drosophila* spermatocytes arise in syncytial cysts, undergo meiosis and differentiate in a spatially ordered progression (reviewed by Fuller, 1993; Lindsley and Tokuyasu, 1980). Mature coiled spermatids are individualized before transfer into the seminal vesicle; mutations affecting spermatid differentiation typically arrest spermatogenesis before this step. To determine if mutations with general mechanosensory defects also disrupt spermatogenesis, we examined sperm production in 1- to 2-day-old males mutant for the *uncoordinated* (*unc*) gene or for several *no-mechanoreceptor-potential* (*nomp*) genes (Kernan et al., 1994). In wild-type males and in *nompA*, *nompB*, *nompC* and *rempA* mutants, individualized sperm accumulate in the seminal vesicles, and are motile when released. However, in *unc* mutants the seminal vesicles remain empty and motile sperm are never observed. Duplications of the proximal X chromosome that complement the sensory defects of *unc* mutants also complement the spermatogenesis defect.

Early events in spermatogenesis, from meiosis to 'onion' stage spermatids, appear normal in *unc* mutants: uniformly sized spermatid nuclei (data not shown) indicate that meiotic chromosome segregation occurs normally. Labeling of DNA and tubulin shows that *unc* mutant spermatids elongate, begin nuclear condensation and contain microtubules (Fig. 1). However, in mutant elongating spermatid cysts, nuclei are dispersed along the flagellar bundle (Fig. 1A,B). To determine whether the dispersed nuclei had separated from the flagella or if intact spermatids had moved relative to each other, we labeled wild-type and mutant testes with an antibody to γ-tubulin. In wild-type spermatids, this antibody labels the junction between the nucleus and flagellum (Wilson et al., 1997). The labeled structure is probably the centriole adjunct, a collar that surrounds the basal body and transforms from a thin sheath to a torus during spermatid elongation (Tates, 1971). Nuclei were frequently separated from centriole adjuncts in mutants, suggesting that the connection between them is indeed disrupted (Fig. 1C). Electron microscopy shows that mutant flagellar axonemes are also defective. Sections of wild-type cysts show the profile of an axoneme and its associated mitochondrial derivative in each of the 64 spermatids in a cyst (Fig. 1D). In *unc* mutants the number of axoneme profiles in each cyst is reduced by an average of 73% (17/64 intact axonemes, n=5). Some of the remaining profiles appear unaffected, but many show defects ranging from a single break to complete disruption of the axoneme into its constituent microtubule doublets (Fig. 1E,F).

To look for ciliogenesis defects in mutant sensory neurons, we visualized ciliary outer segments in chordotonal organs and olfactory bristles with a membrane-associated GFP, mCD8-GFP (Lee and Luo, 1999) (Fig. 2A-F). In wild-type neurons (Fig. 2A,B,E) this protein outlines a cilium extending from each sensory process. In *unc* mutants (Fig. 2C,D,F), these cilia are absent or deformed. Comparing the ultrastructure of wild-type and mutant chordotonal organs (Fig. 2G-L) shows missing or truncated cilia in *unc* mutants. Transverse sections of ciliary bases show some broken rings (Fig. 2I), indicating that the distal basal bodies are also disrupted. The proximal basal

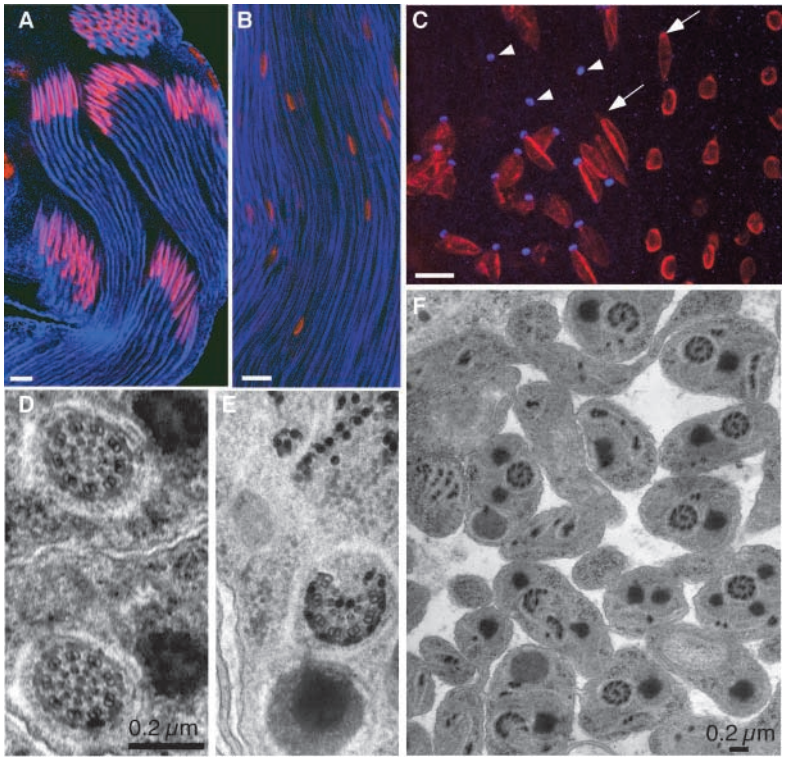

Fig. 1. Spermatogenesis defects in *unc* mutants. (A,B) Cysts of elongating spermatids in wild-type (A) and *unc* mutant (B) testis, stained for nuclei (red) and β-tubulin (blue). Nuclei are clustered at the head of wild-type cysts but are dispersed in *unc* mutants. (C) Nuclei in cysts of an *unc* mutant testis, stained for DNA (red) and γ-tubulin (blue). Two stages of nuclear condensation are present. Earlier, less-condensed nuclei (left side of panel) are still associated with the γ-tubulin-containing centriole adjuncts as in wild type, but mutant nuclei (arrows) and adjuncts (arrowheads) frequently detach at later stages. Mutant nuclei do not condense further than the stage seen in cross-section on the right. (D-F) Ultrathin sections of wild-type (D) and mutant (E,F) testes. Wild-type spermatids have a canonical 9+2 axoneme, associated with an electron-dense mitochondrial derivative. Most mutant axonemes are partially or completely disrupted, and lose their tight association with mitochondrial derivatives. Scale bars: in A-C, 5 μm; in D,F, 0.2 μm.

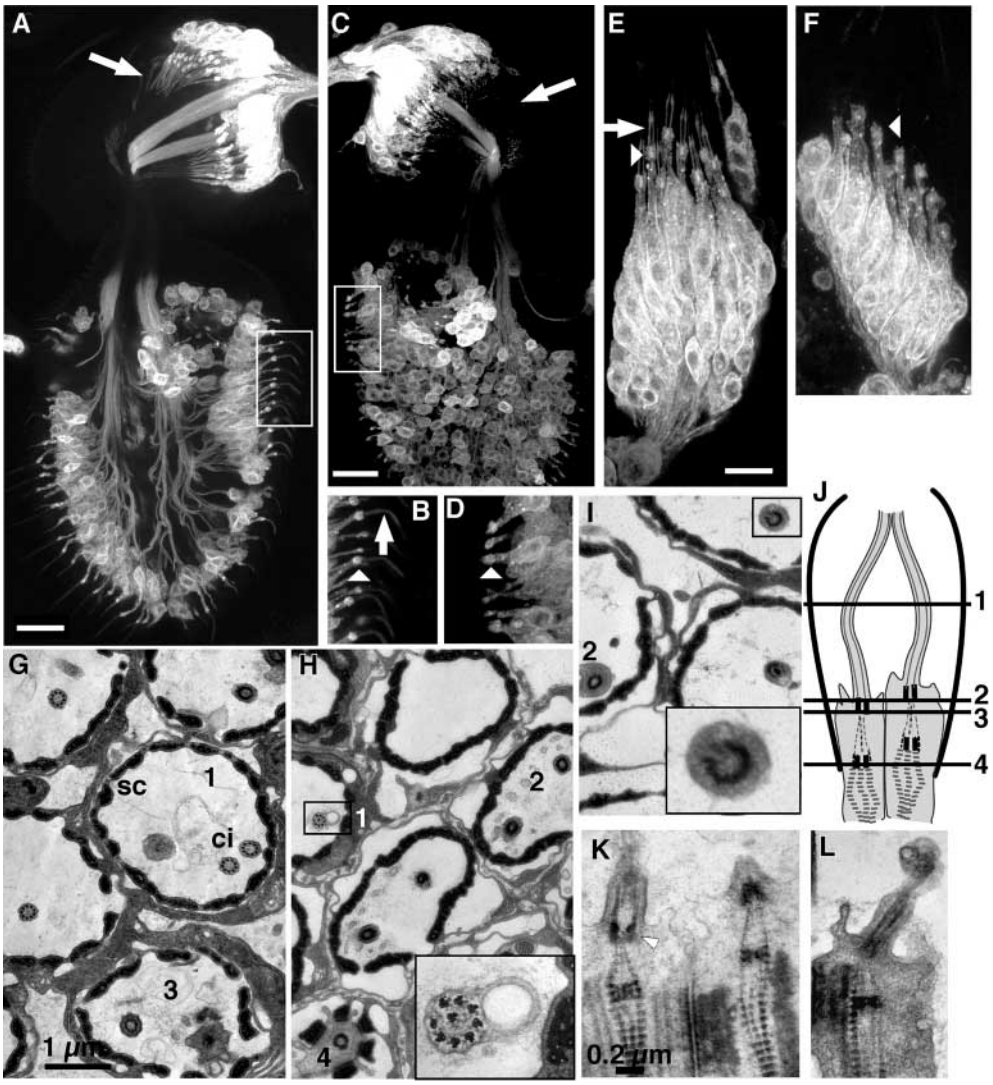

Fig. 2. Defective sensory cilia in *unc* mutants. (A-F) Sensory neurons in the antenna (A-D) and the femoral chordotonal organ (E,F), labeled by neuronal expression of mCD8-GFP. Arrows indicate ciliary outer dendritic segments, and arrowheads to the tips of the inner dendritic segments. In wild type, cilia extend from sensory processes of olfactory neurons on the antenna (A, enlarged in B) and femoral chordotonal neurons (E). In *unc* mutants (C,D,F) neurons and inner sensory processes are still present, but the cilia are missing or truncated. (G-L) ultrathin sections of individual sensory units (scolopidia) in chordotonal organs. (G) Transverse sections of wild-type scolopidia, showing profiles of two cilia (ci) enclosed in each scolopale (sc). (H,I) *unc* mutant femoral (H) or antennal (I) scolopidia with missing or disrupted cilia (box and inset). Sections through some basal bodies (I) also showed breaks (inset). (J) Schematic of a scolopidium, relating numbered section planes to the sections seen in G-I. (K,L) Longitudinal sections of wild-type and mutant ciliary bases. Basal bodies appear as paired electron-dense structures (arrowhead); the distal basal body was often less clearly defined in mutant cilia. Scale bars: 20 μm in A,C; 5 μm in E; 1 μm in G; 0.2 μm in K.

bodies, ciliary rootlets and non-neuronal sensory structures are not visibly affected.

Positional cloning and protein structure

unc lies within the overlap of the X chromosomal deficiencies *Df(1)S54* and *Df(1)B57*. Phage clones from this interval (Healy et al., 1988) hybridized to the P1 clone DS04081; subcloned probes were used to locate the endpoint of *Df(1)S54* (Fig. 3A). cDNA library screening (data not shown) and genomic sequence annotations (Adams, 2000) identified seven transcription units in the interval between the deficiency endpoint and a stretch of repetitive DNA. Rearrangements associated with the X-ray induced mutations unc^{2}, unc^{17} and unc^{24} were found to cluster within 2 kb (Fig. 3A). The genomic DNA encompassing these breakpoints matched a single expressed sequence tag, LP08350, from the *Drosophila* genome project. The corresponding cDNA was sequenced and extended by 5′-RACE to give a predicted transcript length of 4464 bp (Fig. 3B). An unc^{+} transgene was constructed from a genomic fragment that includes 2kb of upstream sequence, joined in the third predicted *unc* exon to the balance of the cDNA. This construct complemented the mutant behavioral, electrophysiological (Fig. 3C) and sterility defects in germline transformants.

The *unc* transcript contains a 1386-amino acid ORF (Fig. 3D). Five EMS-induced *unc* alleles were found to have single-base changes creating premature stop codons in the first half of the ORF. The COILS program (Lupas et al., 1991) identified five coiled-coil segments, bounded by proline residues or a proline-rich region. A motif (GALNVGKT; conserved residues underlined) similar to a nucleotide-binding P-loop but lacking the usual preceding hydrophobic residues begins at residue 816. Two mutations of this motif (G816E and K822A) were separately made in the rescue construct. Both mutated transgenes complemented the *unc* spermatogenesis and sensory defects (data not shown), indicating that nucleotide binding or hydrolysis at this site is not required for UNC function.

Sequence similarity searches indicate that *unc* is unique in the *D. melanogaster* genome; the closest matches are to other coiled-coil proteins. Homologs of *unc* are currently found only in dipteran insects. A predicted *unc* homolog appears in *D. pseudoobscura* (*D. pseudoobscura* sequencing project; http://www.hgsc.bcm.tmc.edu/projects/drosophila/), but shows

only 31% amino acid identity with UNC, unusually low for this closely related species (~50 Mya divergence). The genome of the mosquito *Anopheles* (Holt et al., 2002), which diverged from *Drosophila* ~240 Mya, includes an unannotated gene (segment AAAB01008986_326) with limited sequence similarity to the N-terminal half of UNC (39% identity over 119 amino acids**)**. Thus, the UNC protein sequence appears to be diverging rapidly, even within the Diptera. The 120-amino acid region that is most highly conserved between all three proteins includes a Lissencephaly 1 homology (LisH) domain (Emes and Ponting, 2001), a short α-helical motif present in several microtubule-associated proteins.

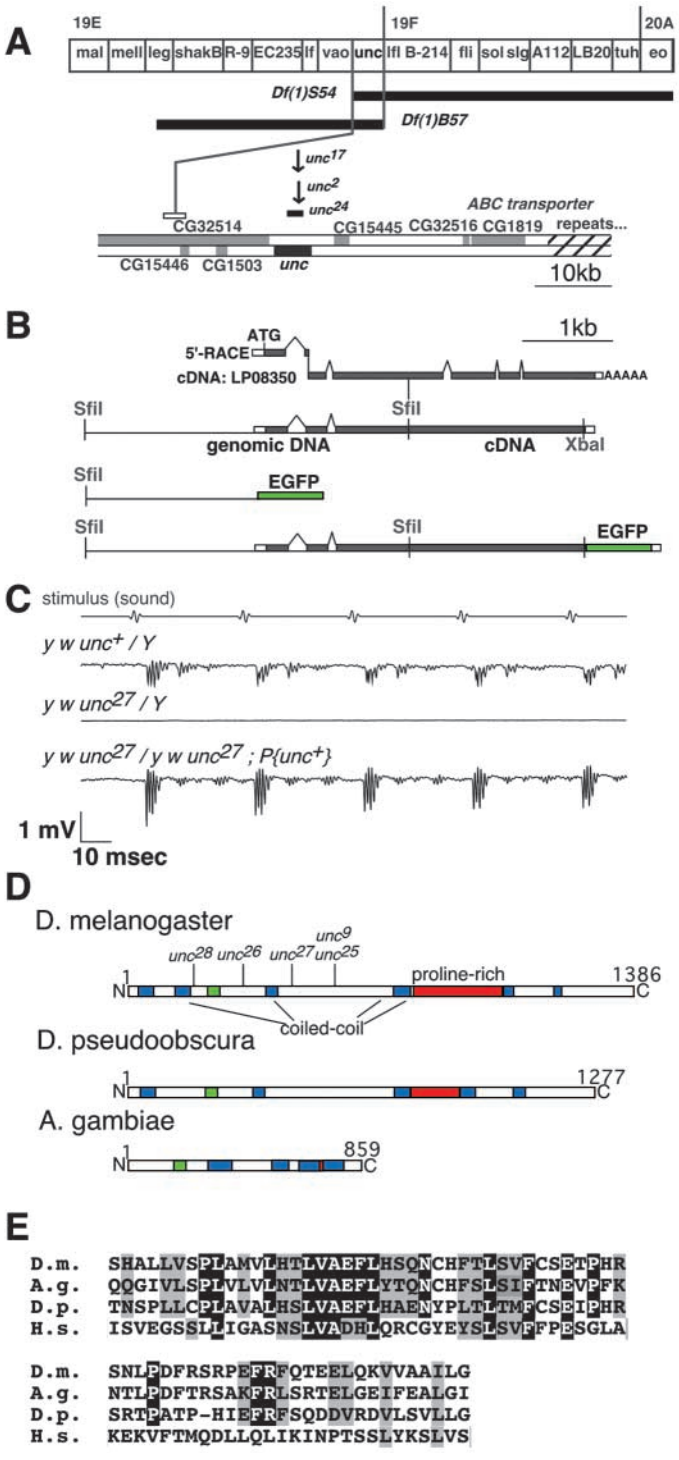

Expression and protein localization

Direct detection of transcripts with an antisense probe showed weak labeling near the apical end of the testis (data not shown). Transcripts in the embryonic PNS were not detectable by in situ hybridization, so to visualize *unc* transcription the upstream region and promoter from the rescue construct (Fig. 3B) was joined to the coding region for enhanced green fluorescent protein (EGFP). In transgenic flies, this construct labels cells close to but not at the apical tip of the testis (Fig. 4A), the location of late gonial cells and early spermatocytes in which most germline transcription occurs. In embryos (Fig. 4B,C) the promoter fusion is expressed in sensory neurons of the PNS, but not in the central nervous system or non-neuronal tissues. During pupal development, expression was observed in sensory neurons of imaginal discs (Fig. 4D,E).

To locate UNC in vivo, a GFP tag was appended to the open reading frame in the *unc*$^{+}$ rescue construct. When crossed into an *unc* mutant genotype, this *unc-GFP* transgene rescued the mechanosensory and male-fertility defects (data not shown), indicating that the fusion protein retains its normal function. In the peripheral nervous system, UNC-GFP is expressed only in ciliated sensory neurons of type I sensilla (Fig. 5), including mechanosensory and olfactory bristles (Fig. 5 A-C) and chordotonal organs (Fig. 5D). In mechanosensory bristles, UNC-GFP labels dots less than 1 μm in diameter close to the tips of the sensory dendrites; several dots are resolved in multiply innervated olfactory bristles. The GFP signal decreased in late (50-75 hours) pupae and was undetectable in adults. No UNC-GFP labeling was observed in photoreceptors or in any somatic cell other than ciliated sensory cells. Counterstaining with anti-HRP, which labels both inner and outer segments, suggests that the GFP-labeled structure is located at their juncture – the position of the basal bodies (Fig. 5A). Larval chordotonal organs stained with the monoclonal antibody 22C10, which labels the inner but not the ciliary outer segment of the sensory process, show two GFP-labeled structures in each neuron. The more proximal abuts the distal

Fig. 3. *unc* encodes a large coiled-coil protein. (A) Complementation and physical maps of the *unc* region at the base of the X chromosome. Flies heterozygous for the overlapping deficiencies *Df(1)S54* and *Df(1)B57* show an *unc* phenotype. The left breakpoint of *Df(1)S54* and breakpoints associated with three x-ray-induced *unc* alleles are indicated. (B) The *unc* transcription unit, with promoter fusion, rescuing transgene and GFP fusion constructs below. The open reading frame of a cDNA clone (LP08350) was extended by 5′-RACE to a 5′ UTR with in-frame stop codons. A transgene including 2 kb of upstream DNA fused to the balance of the cDNA restored normal sound-evoked responses (C) to *unc* mutants. The same upstream DNA fragment was fused to EGFP to report transcription from the *unc* promoter. To examine protein localization, DNA encoding EGFP was appended to the *unc*-coding sequence. (D) Predicted *unc* proteins from *D. melanogaster* (D.m.), *D. pseudoobscura* (D.p.) and the mosquito *Anopheles gambiae* (A.g.). Each protein includes several short coiled-coil segments, separated by proline residues or proline-rich regions, and a Lissencephaly 1 homology (LisH) motif (green box). The positions of stop codons in five EMS-induced *unc* alleles are indicated in the *melanogaster* protein. (E) Alignment of the LisH motifs from the proteins in D and from the human ODF1 protein (H.s.).

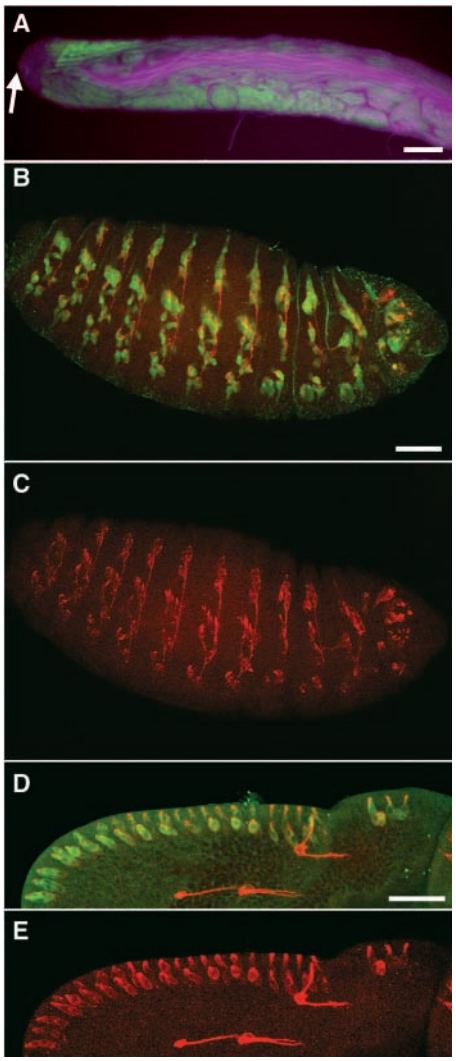

Fig. 4. *unc*-driven GFP expression in testes and sensory neurons. (A) Apical end of adult testis with GFP fluorescence (green) and autofluorescence from spermatid mitochondria (blue). The *unc* promoter region drives visible GFP expression in spermatocytes, but not in the early gonial or stem cells at the apical tip (arrow). (B-E) GFP expression in peripheral sensory neurons of the embryo (B,C) and pupal wing margin (D,E), visualized with anti-GFP (green) and the neuronal marker Futsch (MAb22C10, red). *unc* is also expressed in the campaniform sensilla of the wing blade, but these cells appear red because of strong expression of Futsch. Scale bars: 40 μm.

extent of 22C10 labeling, so these structures probably correspond to the proximal and distal basal bodies.

In adult testes, an UNC-GFP signal is visible adjacent to the clustered heads of elongating spermatids (Fig. 6A). The GFP-labeled structures appear rod-shaped in early spermatids (Fig. 6B), and collar-shaped in elongating spermatids (Fig. 6C), suggesting localization to the centriole adjunct. In late spermatids with fully-condensed nuclei, UNC-GFP disappears or is delocalized (Fig. 6C).

Surprisingly, UNC-GFP is localized to the paired centrioles of dividing spermatocytes undergoing the first meiotic division (Fig. 6D). Identification of these GFP-labeled structures as centrioles was confirmed by visualizing the centrosomal protein centrosomin (Li and Kaufman, 1996). A testis-specific centrosomin isoform is expressed in the male germline, through the early stages of spermatid differentiation and is localized to the centrosome in dividing cells (Li, 1998). Like UNC, centrosomin is expressed, but not specifically localized, in gonial cells near the tip of the testis (Fig. 6E,F). In UNC-GFP-expressing spermatocytes undergoing meiosis I, anti-centrosomin surrounds the proximal end of each GFP-labeled rod (Fig. 6G).

The stability of the UNC-GFP association with centrioles was assessed by fluorescence recovery after photobleaching (FRAP). One of a pair of centrioles in cultured primary or

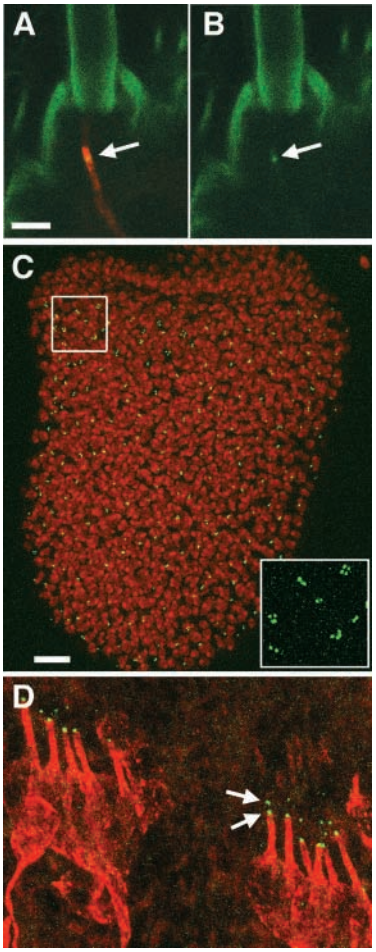

Fig. 5. UNC-GFP localization in sensory neurons. (A,B) A singly innervated macrochaete bristle showing a focus of Unc-GFP labeling (arrow) near the end of the sensory process. The neuronal process and the ciliary outer segment are labeled with anti-HRP (red); autofluoresence from the cuticle outlines the bristle and socket in green. (C) Clustered spots of Unc-GFP (green) label the multiply innervated olfactory sensilla on the third antennal segment. Nuclei are labeled with propidium iodide (red). The boxed region is enlarged in the inset, without the nuclear labeling. (D) Two embryonic lateral chordotonal clusters. Anti-22C10 (red) labels the neuronal and inner dendritic segments, but not the ciliary outer segments. Each neuron shows two labeled spots (green, arrows), with the more proximal at the end of the inner segment. Scale bars: in A, 1 μm for A,B; in C, 20 μm for C, 4 μm for D.

secondary spermatocytes was bleached and the pair was monitored for recovery of GFP fluorescence. Little or no fluorescence recovery was observed in eight experiments, up to an hour after bleaching, indicating that once UNC is bound to centrioles, it does not exchange rapidly between centrioles and cytoplasm.

UNC-GFP localization in maturing and arrested spermatocytes

To specify when UNC-GFP first becomes localized to centrioles in the germline, we examined its localization in larval testes, which consist mostly of gonial cells and maturing spermatocytes. Localized UNC-GFP first appears in early spermatocytes as two pairs of equally labeled dots, which increase in length as the spermatocytes mature, ultimately migrating to the cell periphery (Fig. 7A-G). This progression mirrors that described for spermatocyte centrioles (Fuller, 1993; Tates, 1971). To confirm the stage at which UNC was localized, we expressed UNC-GFP in mutants that arrest spermatogenesis before and during spermatocyte differentiation. *bag-of-marbles* (*bam*) and *benign gonial cell neoplasm* (*bgcn*) mutants accumulate amplifying gonial cells (Gonczy et al., 1997). In these cells (Fig. 7H,I), no localized UNC-GFP is observed. *spermatocyte arrest* (*sa*) mutants accumulate large spermatocytes that are arrested before the first meiotic division (Lin et al., 1996). UNC-GFP is localized to paired centrioles in *sa* mutants, but the labeled area does not increase to the wild-type extent, and the centrioles do not migrate to the cell periphery (Fig. 7J,K). Taken together with the results from wild-type testes, these data indicate that UNC is produced during gonial cell proliferation and in early spermatocytes, but is not localized until after centriole duplication in early G2, when it associates equally with all four centrioles.

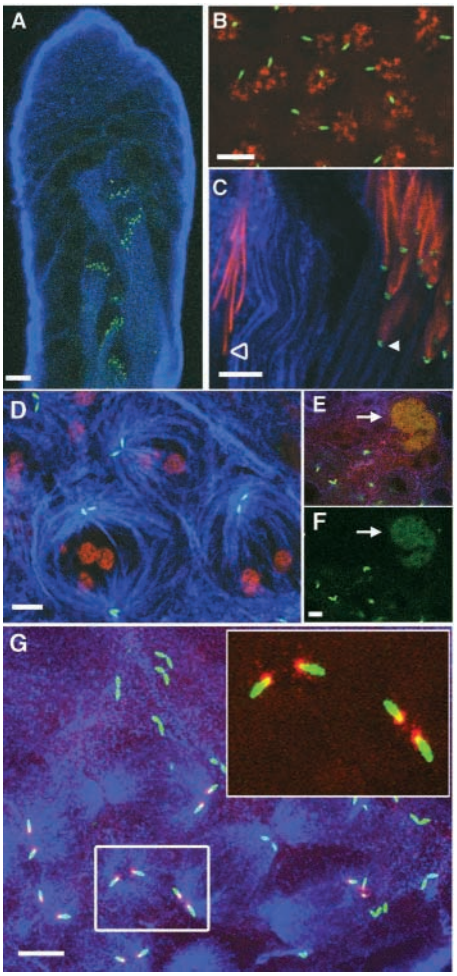

Fig. 6. Unc-GFP localization in spermatogenesis. Confocal images of spermatids (A-C) and spermatocytes or gonial cells (D-G) expressing UNC-GFP (green). Anti-β-tubulin (blue) labels axonemal and cytoplasmic microtubules in all panels, and propidium iodide (red) stains DNA in B-D. (A) Low-magnification image of the of the testis tip, showing UNC-GFP in elongated spermatids at the apical end of the flagella. (B) Round spermatids immediately following meiosis II show a single GFP-labeled centriole associated with each nucleus. (C) UNC-GFP is associated with the centriole adjunct (arrowhead) in elongating spermatids, but is not present in mature spermatids with fully condensed nuclei (open arrowhead). (D) Primary spermatocytes in meiosis I, showing paired centrioles at each pole of the meiotic spindle. (E,F) Co-expression of UNC-GFP and centrosomin (red) in gonial cells (arrow). (G) Colocalization of UNC-GFP and centrosomin (red) in dividing spermatocytes. Scale bars: 10 μm in A; 5 μm in B-G.

Reduced γ-tubulin colocalization and centriole length in *unc* mutants

γ-Tubulins form part of a ring complex that nucleates and anchors microtubule minus ends at centrosomes (Moritz et al., 1998). In gonial and meiotic divisions of spermatogenesis, one γ-tubulin isoform, γTub23C, localizes to foci at the spindle poles (Wilson et al., 1997). The proximal ends of the Unc-GFP-labeled centrioles are embedded in these foci. In mature spermatocytes, anti-γTub23C labels v-shaped structures that enclose and connect the proximal ends of a pair of centrioles. In postmeiotic spermatids, γTub23C and UNC-GFP labeling behave similarly, first condensing to the centriole adjunct (Wilson et al., 1997) and finally disappearing in mature sperm (data not shown).

We examined the localization of centrosomin and gamma-tubulin in *unc* mutants. Centrosomin labeling was unchanged suggesting that, consistent with the absence of cytological meiotic defects, the centrosomes in dividing spermatocytes form and segregate normally. However, the γ-tubulin-labeled structures in larval spermatocytes were altered in mutants: the v-shaped structures were reduced to dots (Fig. 8B,C). This suggests that either the centriole pairs themselves or the areas to which γ-tubulin binds are much reduced.

To determine if the reduced γ-tubulin labeling reflected altered centriole structure in *unc* mutants, we examined centriole ultrastructure in larval spermatocytes. Long, bipartite centrioles characteristic of spermatocytes (Gonzalez et al., 1998; Tates, 1971) were seen in wild-type cells (Fig. 9A). Transverse sections of the proximal ends showed nine microtubule triplets, while longitudinal sections showed differentiated distal ends enclosed in electron-dense, membranous sheaths. In *unc* mutants, similar transverse and longitudinal profiles were seen, including nascent distal sections and sheaths (Fig. 9B). However, longitudinally sectioned centrioles in *unc* mutants were shorter than in wild type: a comparison of 11 mutant and 13 wild-type centrioles (Fig. 9C) shows both proximal and distal sections being

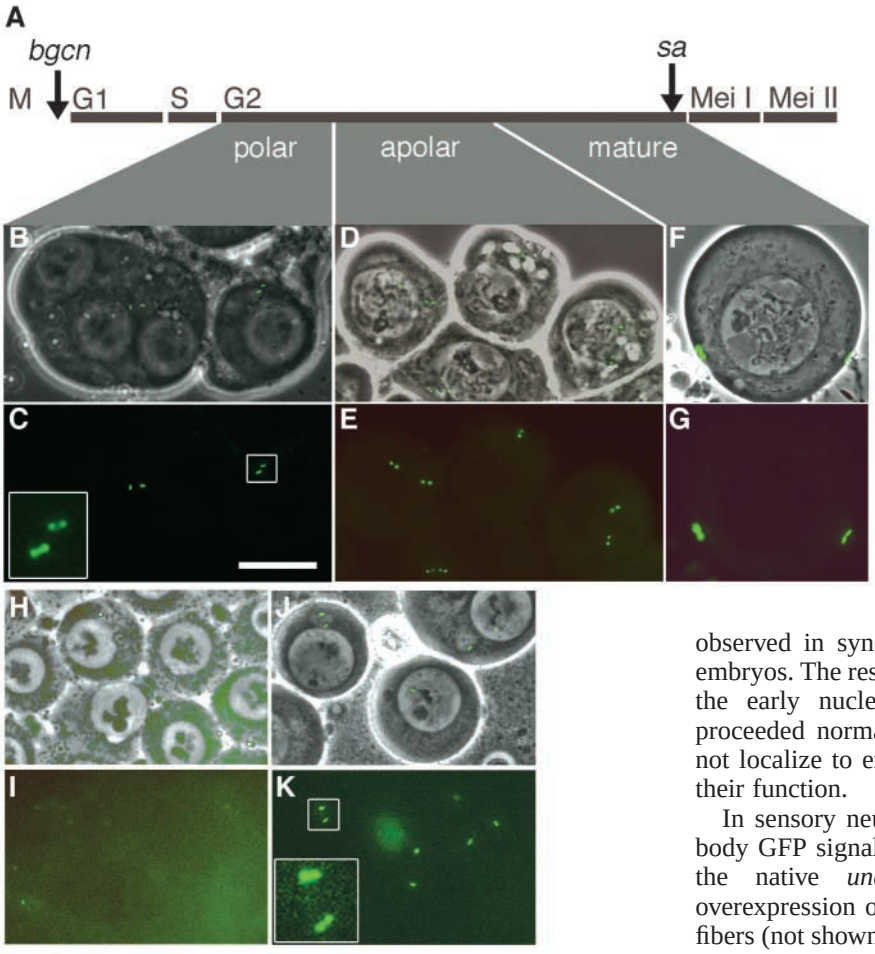

Fig. 7. Unc-GFP is first localized in G2 spermatocytes. Merged phase-contrast and fluorescence image of spermatocytes from larval testes expressing UNC-GFP. (A) Timeline of spermatocyte development. (B-G) Polar, apolar and mature spermatocytes in a wild-type testis. UNC-GFP is first localized in polar spermatocytes to four paired dots (B,C; enlarged in inset); the labeled structures are larger in apolar spermatocytes (D,E) and migrate to the cell periphery in mature cells (F,G). (H,I) Arrested gonial cells in *bgcn* mutant testis: no localized Unc-GFP is detectable. (J,K) Arrested primary spermatocytes in an *sa* mutant: paired UNC-GFP labeled structures are smaller than those in wild-type cells at a comparable stage. Scale bar: 20 μm.

reduced in mutants. Together with the altered γ-tubulin labeling, these data show that *unc* mutant centrioles are defective even before meiosis, although the cellular consequences are not seen until spermatid elongation.

Unc binds centrioles only in ciliogenic cells

To investigate the cellular contexts in which Unc is localized and functions, we used a GAL4 transcription factor to drive transcription of full-length, GFP-tagged *unc* cDNA from an upstream activation sequence (UAS) (Brand and Dormand, 1995) in neurons and other somatic cells. Expressing UNC-GFP in neurons of *unc* mutant flies rescues their behavioral phenotype, but not their spermatogenesis defect. Surprisingly, three independent *UASunc-GFP* inserts rescue the *unc* mutant behavioral defects, but not the spermatogenesis defect, in the absence of any GAL4 driver. Either the cDNA includes sequences that normally regulate neuronal transcription, or a basal *unc* expression level is sufficient for function in sensory neurons.

Only spermatocytes and sensory neurons, postmitotic cells that construct basal bodies and cilia, normally express *unc*. To investigate if ectopic UNC expression interferes with mitotic centrioles and centrosomes, we crossed males carrying *UASunc-GFP* to females expressing *GAL4* in the germline (Tracey et al., 2000), to generate embryos containing high levels of UNC-GFP. No centrosomal GFP localization was observed in syncytial embryos (not shown) or cellularizing embryos. The resulting larvae were fully viable, indicating that the early nuclear divisions and later cell divisions had proceeded normally. Thus, ectopically expressed UNC does not localize to embryonic mitotic centrioles or interfere with their function.

In sensory neurons, the *unc-GFP* cDNA produces a basal body GFP signal similar to that obtained by expression from the native *unc* promoter (not shown). GAL4-driven overexpression of UNC-GFP in other tissues including nerve fibers (not shown), salivary gland, tracheal cells and epidermal cells illuminates filamentous structures ranging from single fibers in nerves to elaborate meshworks extending throughout salivary gland cells. These could be endogenous structures labeled by ectopic UNC-GFP, or artifacts of UNC-GFP aggregation: similar filaments have been observed to result from the concentration or overexpression of other coiled-coil proteins (e.g. septins) (Trimble, 1999). In any case, the GFP-labeled filaments have no evident phenotypic effects: flies overexpressing *unc-GFP* developed, behaved and reproduced normally.

Discussion

unc mutants exemplify a general ciliogenesis defect in *Drosophila*

Mutations affecting ciliogenesis have been identified in eukaryotes ranging from algae to mammals. Their phenotypes reflect the functions that cilia perform in each organism, and range from motility and signaling defects in *Chlamydomonas*, to situs inversus, skeletal defects, male-sterility and cyst formation in mammals. The *unc* mutant phenotypes reveal the results of a general failure of ciliogenesis in *Drosophila*: a combination of sensory and spermatogenesis defects reflecting a requirement for normal ciliary differentiation in type I sensory neurons and in spermatids. Though similarly based on axonemal structures, sensory cilia and sperm flagella differ in form and molecular composition. Many male-sterile mutations of *Drosophila* specifically affect spermatid axonemes (Fuller,

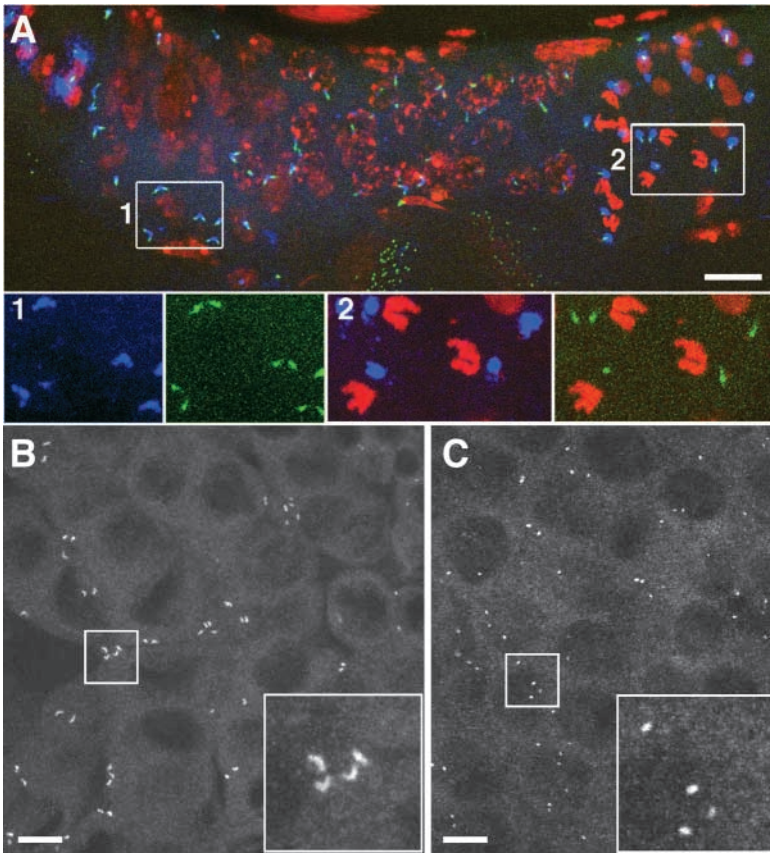

Fig. 8. Altered γ-tubulin localization in *unc* mutant spermatocytes. (A) Unc-GFP (green) and anti-γ-tubulin (blue) labeling cysts at multiple stages of development in a wild-type testis. DNA is labeled with propidium iodide (red). Boxes, enlarged below, include cells entering meiosis I (1) and exiting meiosis II (2). (B,C) γ-Tubulin labeling in wild-type (B)and *unc* mutant (C) spermatocytes. In mutants, γ-tubulin staining is reduced to small dots, each probably equivalent to a pair of centrioles in wild type. Scale bars: 10 μm.

1993; Lindsley and Tokuyasu, 1980). For example, loss of axonemal dynein subunits encoded on the Y chromosome (Carvalho et al., 2000; Kurek et al., 1998; Zhang and Stankiewicz, 1998) leads to male-sterility with immotile spermatids, but neither XO males nor, of course, normal XX females show sensory defects. Conversely, *Drosophila* mutants defective in intraflagellar transport, a conserved protein complex that is required to assemble and maintain axonemal structures in other systems, lack normal sensory cilia but, surprisingly, produce functional sperm (Dubruille et al., 2002; Han et al., 2003; Sarpal et al., 2003). *touch-insensitive-larvaB* (*tilB*) mutants (Eberl et al., 2000) combine sperm axoneme defects with sensory defects specific to chordotonal organs. *unc*, by contrast, functions in all ciliated sensory neurons, as well as spermatids, suggesting that it affects a core ciliogenesis function.

Unc localization and function

unc is expressed only in postmitotic cells that are forming or will form cilia, and it is localized to centrioles in these cells. The stability and persistence of UNC-GFP labeling on the centrioles, from early spermatocytes through meiosis, indicate that it associates more closely with the centriole than do γ-tubulin and centrosomin, which show a more diffuse and cell cycle-dependent association. However, UNC is probably not an integral component of the centriole microtubules, as its later redistribution in maturing spermatids, like that of γ-tubulin, appears to reflect the transformation of an accessory structure, the centriole adjunct, from a sheath to a doughnut-shaped collar. UNC-GFP is cytoplasmic in dividing gonial cells or when ectopically expressed in early embryos, while it forms large, apparently artefactual aggregates when overexpressed in differentiated somatic cells. Therefore, specific modifications of the centrioles or of UNC itself must regulate its normal localization in neurons and spermatocytes.

What does UNC do? Centrosome organization and replication, the functions of centrioles in dividing cells, are not affected in *unc* mutants: γ-tubulin and centrosomin are still recruited to the meiotic centrosomes, bipolar spindles form and meiosis proceeds normally. Abnormalities in *unc* mutants are restricted to axonemal structures, implying a specific defect in basal body function. Basal bodies are present and correctly located in mutant sensory neurons, but show ultrastructural defects and fail to template normal axonemes. Similar defects are caused by mutations affecting intraflagellar transport (IFT) in *Chlamydomonas*, nematodes and mammals (Haycraft et al., 2001; Pazour et al., 2000). IFT is required for the assembly and maintenance of flagella and cilia, and involves transport of a protein complex along axonemes by kinesin II (reviewed by Rosenbaum and Witman, 2002). However, UNC is not part of the core IFT mechanism. IFT particle proteins, unlike UNC, are well-conserved across eukaryotic phyla, including *Drosophila* (Han et al., 2003). *Drosophila* IFT complexes are present along sensory cilia (Han et al., 2003), while UNC-GFP appears only at the basal body. Finally, IFT is not needed to assemble *Drosophila* sperm flagella: mutants lacking the *Drosophila* homolog of the IFT88 protein (Han et al., 2003), or with defects in the kinesin II accessory protein (Sarpal et al., 2003) have defective sensory cilia but normal sperm.

UNC could, however, recruit IFT particles or other axoneme components to the basal body for export to cilia. Its sequence is consistent with such a role. The coiled-coil segments that are its main structural motifs are a common feature of multiprotein complexes, including centrosome and spindle pole body proteins. The several separate segments in UNC may enable it to bring together multiple coiled-coil protein partners, while the aggregates produced by UNC overexpression suggest that it may self-associate. UNC shares a conserved, partial lissencephaly homology (LisH) motif with a number of proteins involved in microtubule organization (Emes and Ponting, 2001), but the specific function of this motif is unknown. In humans, the gene mutated in oral-facial-digital syndrome (*OFD1*), a probable ciliary disorder, encodes a protein with a similar arrangement of a LisH domain and coiled-coil segments, which is localized to centrosomes (Ferrante et al., 2001; Romio et al., 2003). OFD1 may therefore have a basal body function similar to that of UNC. However,

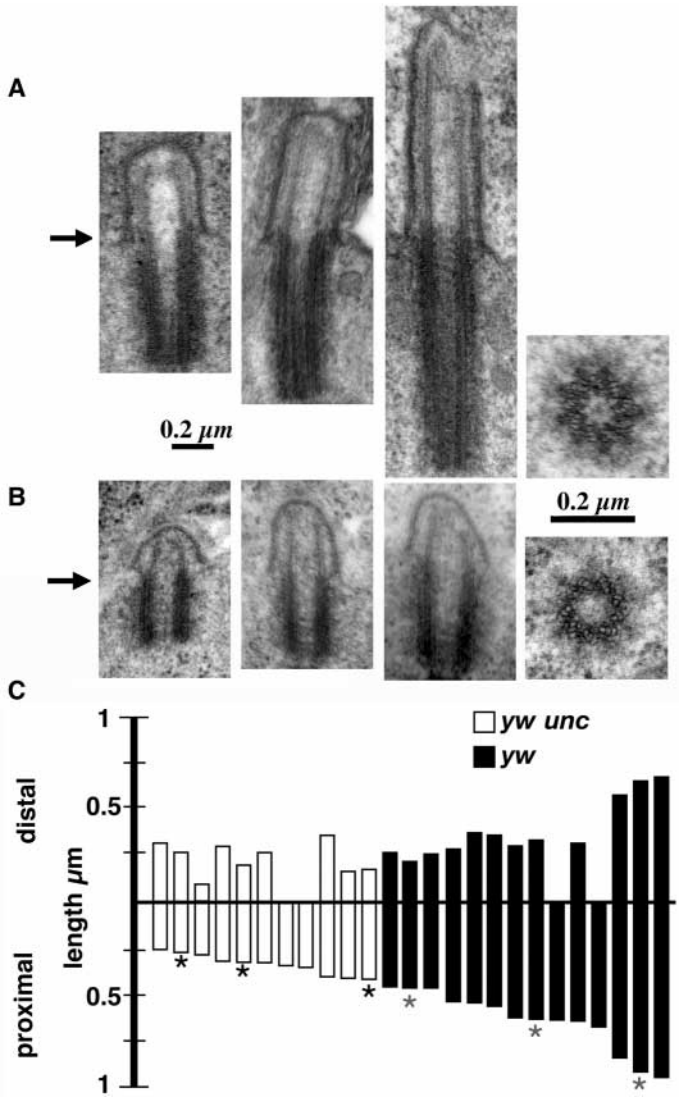

Fig. 9. Reduced centrioles in *unc* mutant spermatocytes. Transverse and longitudinal sections of centrioles in (A) wild-type (*y w*) and (B) mutant (*y w unc*) spermatocytes show similar ultrastructure with microtubule triplets, but both the proximal and distal sections of mutant centrioles are shorter. (C) Lengths of the proximal and distal parts of longitudinally sectioned centrioles. Asterisks indicate the centrioles shown in A and B.

OFD1 failed to rescue *unc* mutant sensory defects when expressed from a transgene in *Drosophila* sensory neurons (data not shown).

UNC and centriole maturation; a comparison with vertebrates

Centrioles in *Drosophila* embryos and most somatic cells are composed of doublet microtubules, lack appendages and do not form cilia (Gonzalez et al., 1998). Their relatively simple structure, and the absence of structural distinctions between mother and daughter centrioles suggest that they are 'neotenous' – i.e. reproduce without undergoing the final stages of maturation (Callaini et al., 1997). This is consistent with the absence of some otherwise conserved centrosomal proteins from *Drosophila* and other ecdysozoa. For example, δ- and ε-tubulins, which are conserved from mammals to *Chlamydomonas* and required for basal body assembly and ciliogenesis (Dutcher and Trabuco, 1998; Chang and Stearns, 2000; Dutcher et al., 2002; Chang et al., 2003), are absent from the sequenced *Drosophila*, *Anopheles* and *Caenorhabditis* genomes. Ninein and cenexin, proteins that identify the ciliogenic centriole in mammals (Mogensen et al., 2000; Piel et al., 2000), are also absent from *Drosophila*. However, *Drosophila* spermatocyte centrioles are complex, with triplet microtubules and, differentiated distal segments that are, in effect, short primary cilia (Gonzalez et al., 1998). Other insect spermatocytes have more elongated flagella associated with centrioles before and during meiosis, a feature that first established the identity of centrioles with basal bodies (Meves, 1900). Spermatocyte and sensory neuron centrioles may be the only centrioles in the fly comparable with mature ciliogenic centrioles in vertebrates, and UNC may substitute for one or more of the proteins that distinguish the ciliogenic centriole in other systems.

The cilium on a mammalian monociliated cell forms in G1, specifically on the older of the two centrioles in a cell. By contrast, all four centrioles in *Drosophila* spermatocytes appear to be equivalent by the time they differentiate: all migrate to the cell periphery and form ciliary extensions. UNC first localizes to spermatocyte centrioles after they have duplicated, and binds equally to all four centrioles. This may reflect a difference between vertebrate and invertebrate ciliogenesis. Alternatively, it may reveal a general uncoupling of centriole duplication and maturation from the cell division cycle in the extended G2 phase that precedes meiosis. In sensory neurons, UNC-GFP is localized to both the proximal and distal basal bodies, both of which are located at the base of the cilium and aligned with its axis. It will be of interest to determine when UNC is first expressed and localized in the neuronal cell lineage.

In summary, UNC is required for ciliogenesis, and its localization is an early marker for the conversion of a mitotic centriole into a ciliogenic basal body. Finding the proteins that interact with UNC to localize it on centrioles and mediate its function will be a key to understanding this remarkable transformation, and how it is regulated during entry into meiosis and neuronal differentiation.

We thank Dr George G. Miklos for phage DNA that provided the initial entry point into the *unc* region; Dr Thomas Kaufman and Dr Patricia Wilson for antibodies; Dr Gail Mandel for confocal microscopy and sequencing facilities; and Ms Wendy Akmentin and Dr Simon Halegoua for assistance with electron microscopy. This project was funded by a postdoctoral training grant and an NRSA fellowship to J.B.; and grants to M.K. from the National Institute for Deafness and Communicative Disorders, and from the Pew Scholars' Program in the Biomedical Sciences.

References

Adams, M. D., Celniker, S. E., Holt, R. A., Evans, C. A., Gocayne, J. D., Amanatides, P. G., Scherer, S. E., Li, P. W., Hoskins, R. A., Galle, R. A. et al. (2000). The genome sequence of Drosophila melanogaster. *Science* **287**, 2185-2195.

Ansley, S. J., Badano, J. L., Blacque, O. E., Hill, J., Hoskins, B. E., Leitch, C. C., Kim, J. C., Ross, A. J., Eichers, E. R., Teslovich, T. M. et al. (2003).

Basal body dysfunction is a likely cause of pleiotropic Bardet-Biedl syndrome. *Nature* **425**, 628-633.
Ashburner, M. (1989). Drosophila*: A Laboratory Manual*. Cold Spring Harbor: Cold Spring Harbor Laboratory Press.
Beisson, J. and Wright, M. (2003). Basal body/centriole assembly and continuity. *Curr. Opin. Cell Biol.* **15**, 96-104.
Bornens, M. (2002). Centrosome composition and microtubule anchoring mechanisms. *Curr. Opin. Cell Biol.* **14**, 25-34.
Brand, A. and Dormand, E. (1995). The GAL4 system as a tool for unravelling the mysteries of the Drosophila nervous system. *Curr. Opin. Neurobiol.* **5**, 572-578.
Callaini, G. and Riparbelli, M. G. (1996). Fertilization in Drosophila melanogaster: centrosome inheritance and organization of the first mitotic spindle. *Dev. Biol.* **176**, 199-208.
Callaini, G., Whitfield, W. G. and Riparbelli, M. G. (1997). Centriole and centrosome dynamics during the embryonic cell cycles that follow the formation of the cellular blastoderm in Drosophila. *Exp. Cell Res.* **234**, 183-190.
Callaini, G., Riparbelli, M. G. and Dallai, R. (1999). Centrosome inheritance in insects: fertilization and parthenogenesis. *Biol. Cell* **91**, 355-366.
Carvalho, A. B., Lazzaro, B. P. and Clark, A. G. (2000). Y chromosomal fertility factors kl-2 and kl-3 of Drosophila melanogaster encode dynein heavy chain polypeptides. *Proc. Natl. Acad. Sci. USA* **97**, 13239-13244.
Chang, P., Giddings, T. H., Jr, Winey, M. and Stearns, T. (2003). Epsilon-tubulin is required for centriole duplication and microtubule organization. *Nat. Cell Biol.* **5**, 71-76.
Chang, P. and Stearns, T. (2000). Delta-tubulin and epsilon-tubulin: two new human centrosomal tubulins reveal new aspects of centrosome structure and function. *Nat. Cell Biol.* **2**, 30-35.
Chen, Z. (1996). Simple modifications to increase specificity of the 5′ RACE procedure. *Trends Genet.* **12**, 87-88.
Doxsey, S. (2001). Re-evaluating centrosome function. *Nat. Rev. Mol. Cell Biol.* **2**, 688-698.
Dubruille, R., Laurencon, A., Vandaele, C., Shishido, E., Coulon-Bublex, M., Swoboda, P., Couble, P., Kernan, M. and Durand, B. (2002). Drosophila regulatory factor X is necessary for ciliated sensory neuron differentiation. *Development* **129**, 5487-5498.
Dutcher, S. K., Morrissette, N. S., Preble, A. M., Rackley, C. and Stanga, J. (2002). epsilon-tubulin is an essential component of the centriole. *Mol. Biol. Cell* **13**, 3859-3869.
Dutcher, S. K. and Trabuco, E. C. (1998). The UNI3 gene is required for assembly of basal bodies of Chlamydomonas and encodes delta-tubulin, a new member of the tubulin superfamily. *Mol. Biol. Cell* **9**, 1293-1308.
Eberl, D., Hardy, R. and Kernan, M. (2000). Genetically similar transduction mechanisms for touch and hearing in *Drosophila*. *J. Neurosci.* **20**, 5981-5988.
Emes, R. D. and Ponting, C. P. (2001). A new sequence motif linking lissencephaly, Treacher Collins and oral-facial-digital type 1 syndromes, microtubule dynamics and cell migration. *Hum. Mol. Genet.* **10**, 2813-2820.
Ferrante, M. I., Giorgio, G., Feather, S. A., Bulfone, A., Wright, V., Ghiani, M., Selicorni, A., Gammaro, L., Scolari, F., Woolf, A. S. et al. (2001). Identification of the gene for oral-facial-digital type I syndrome. *Am. J. Hum. Genet.* **68**, 569-576.
Fuller, M. (1993). Spermatogenesis. In *The Development of* Drosophila melanogaster, Vol. 2 (ed. M. Bate and A. Martinez Arias), pp. 71-147. New York: Cold Spring Harbor Laboratory Press.
Gloor, G. and Engels, W. (1992). Single-fly DNA preps for PCR. *Drosophila Information Service*. **71**, 148-149.
Gonczy, P., Matunis, E. and DiNardo, S. (1997). bag-of-marbles and benign gonial cell neoplasm act in the germline to restrict proliferation during Drosophila spermatogenesis. *Development* **124**, 4361-4371.
Gonzalez, C., Tavosanis, G. and Mollinari, C. (1998). Centrosomes and microtubule organisation during Drosophila development. *J. Cell Sci.* **111**, 2697-2706.
Han, Y.-G., Kwok, B. H. and Kernan, M. J. (2003). Intraflagellar transport is required in Drosophila to differentiate sensory cilia but not sperm. *Curr. Biol.* **13**, 1679-1686.
Haycraft, C. J., Swoboda, P., Taulman, P. D., Thomas, J. H. and Yoder, B. K. (2001). The C. elegans homolog of the murine cystic kidney disease gene Tg737 functions in a ciliogenic pathway and is disrupted in osm-5 mutant worms. *Development* **128**, 1493-1505.
Healy, M. J., Russell, R. J. and Miklos, G. (1988). Molecular studies on interspersed repetitive and unique sequences in the region of the complementation group uncoordinated on the X chromosome of *Drosophila melanogaster*. *Mol. Gen. Genet.* **213**, 63-71.
Holt, R. A., Subramanian, G. M., Halpern, A., Sutton, G. G., Charlab, R., Nusskern, D. R., Wincker, P., Clark, A. G., Ribeiro, J. M., Wides, R. et al. (2002). The genome sequence of the malaria mosquito Anopheles gambiae. *Science* **298**, 129-149.
Kernan, M., Cowan, D. and Zuker, C. (1994). Genetic dissection of mechanosensory transduction: mechanoreception-defective mutations of Drosophila. *Neuron* **12**, 1195-1206.
Kochanski, R. and Borisy, G. (1990). Mode of centriole duplication and distribution. *J. Cell Biol.* **110**, 1599-1605.
Kurek, R., Reugels, A. M., Glatzer, K. H. and Bunemann, H. (1998). The Y chromosomal fertility factor Threads in Drosophila hydei harbors a functional gene encoding an axonemal dynein beta heavy chain protein. *Genetics* **149**, 1363-1376.
Lange, B. and Gull, K. (1995). A molecular marker for centriole maturation in the mammalian cell cycle. *J. Cell Biol.* **130**, 919-927.
Lange, B. M., Faragher, A. J., March, P. and Gull, K. (2000). Centriole duplication and maturation in animal cells. *Curr. Top. Dev. Biol.* **49**, 235-249.
Lee, T. and Luo, L. (1999). Mosaic analysis with a repressible cell marker for studies of gene function in neuronal morphogenesis. *Neuron* **22**, 451-461.
Li, K. and Kaufman, T. C. (1996). The homeotic target gene centrosomin encodes an essential centrosomal component. *Cell* **85**, 585-596.
Li, K., Xu, E. Y., Cecil, J. K., Turner, F. R., Megraw, T. L. and Kaufman, T. C. (1998). Drosophila centrosomin protein is required for male meiosis and assembly of the flagellar axoneme. *J. Cell Biol.* **141**, 455-467.
Lin, T. Y., Viswanathan, S., Wood, C., Wilson, P. G., Wolf, N. and Fuller, M. T. (1996). Coordinate developmental control of the meiotic cell cycle and spermatid differentiation in Drosophila males. *Development* **122**, 1331-1341.
Lindsley, D. and Tokuyasu, K. T. (1980). Spermatogenesis. In *Genetics and Biology of* Drosophila (ed. M. Ashburner and T. R. Wright), pp. 225-294. New York: Academic Press.
Liu, X., Vansant, G., Udovichenko, I. P., Wolfrum, U. and Williams, D. S. (1997). Myosin VIIa, the product of the Usher 1B syndrome gene, is concentrated in the connecting cilia of photoreceptor cells. *Cell Motil. Cytoskel.* **37**, 240-252.
Lupas, A., van Dyke, M. and Stock, J. (1991). Predicting coiled coils from protein sequences. *Science* **252**, 1162-1164.
Marshall, W. F. and Rosenbaum, J. L. (2000). How centrioles work: lessons from green yeast. *Curr. Opin. Cell Biol.* **12**, 119-125.
Meves, F. (1900). Ueber den von la Valette St. George entdecktden Nebenkern (Mitochondrionkörper) deer Samenzellen. *Archiv für mikroskopische Anatomie und Entwicklungsgeschichte* **56**, 553-606.
Mogensen, M. M., Malik, A., Piel, M., Bouckson-Castaing, V. and Bornens, M. (2000). Microtubule minus-end anchorage at centrosomal and non-centrosomal sites: the role of ninein. *J. Cell Sci.* **113**, 3013-3023.
Moritz, M., Zheng, Y., Alberts, B. M. and Oegema, K. (1998). Recruitment of the gamma-tubulin ring complex to Drosophila salt- stripped centrosome scaffolds. *J. Cell Biol.* **142**, 775-786.
Nakagawa, Y., Yamane, Y., Okanoue, T. and Tsukita, S. (2001). Outer dense fiber 2 is a widespread centrosome scaffold component preferentially associated with mother centrioles: its identification from isolated centrosomes. *Mol. Biol. Cell* **12**, 1687-1697.
Noguchi, T. and Miller, K. G. (2003). A role for actin dynamics in individualization during spermatogenesis in *Drosophila melanogaster*. *Development* **130**, 1805-1816.
Pazour, G. J. and Witman, G. B. (2003). The vertebrate primary cilium is a sensory organelle. *Curr. Opin. Cell Biol.* **15**, 105-110.
Pazour, G. J., Dickert, B. L., Vucica, Y., Seeley, E. S., Rosenbaum, J. L., Witman, G. B. and Cole, D. G. (2000). Chlamydomonas IFT88 and its mouse homologue, polycystic kidney disease gene Tg737, are required for assembly of cilia and flagella. *J. Cell Biol.* **151**, 709-718.
Piel, M., Meyer, P., Khodjakov, A., Rieder, C. L. and Bornens, M. (2000). The respective contributions of the mother and daughter centrioles to centrosome activity and behavior in vertebrate cells. *J. Cell Biol.* **149**, 317-330.
Rieder, C. and Borisy, G. (1982). The centrosome cycle in PtK2 cells: asymmetric distribution and structural changes in the pericentriolar materiel. *Biol. Cell.* **44**, 117-132.
Romio, L., Wright, V., Price, K., Winyard, P. J., Donnai, D., Porteous, M. E., Franco, B., Giorgio, G., Malcolm, S., Woolf, A. S. et al. (2003). OFD1,

the gene mutated in oral-facial-digital syndrome type 1, is expressed in the metanephros and in human embryonic renal mesenchymal cells. *J. Am. Soc. Nephrol.* **14**, 680-689.

Rosenbaum, J. L., Cole, D. G. and Diener, D. R. (1999). Intraflagellar transport: the eyes have it. *J. Cell Biol.* **144**, 385-388.

Rosenbaum, J. L. and Witman, G. B. (2002). Intraflagellar transport. *Nat. Rev. Mol. Cell Biol.* **3**, 813-825.

Rubin, G. M. and Spradling, A. C. (1982). Genetic transformation of Drosophila with transposable element vectors. *Science* **218**, 348-353.

Sarpal, R., Todi, S. V., Sivan-Loukianova, E., Shirolikar, S., Subramanian, N., Raff, E. C., Erickson, J. W., Ray, K. and Eberl, D. F. (2003). Drosophila KAP interacts with the kinesin II motor subunit KLP64D to assemble chordotonal sensory cilia, but not sperm tails. *Curr. Biol.* **13**, 1687-1696.

Schatten, G. (1994). The centrosome and its mode of inheritance: the reduction of the centrosome during gametogenesis and its restoration during fertilization. *Dev. Biol.* **165**, 299-335.

Tates, A. (1971). *Cytodifferentiation during Spermatogenesis in* Drosophila. Leiden: Rijksuniversiteit.

Tautz, D. and Pfeifle, C. (1989). A non-radioactive in situ hybridization method for the localization of specific RNAs in Drosophila embryos reveals translational control of the segmentation gene hunchback. *Chromosoma* **98**, 81-85.

Tracey, W. D., Jr, Ning, X., Klingler, M., Kramer, S. G. and Gergen, J. P. (2000). Quantitative analysis of gene function in the Drosophila embryo. *Genetics* **154**, 273-284.

Trimble, W. S. (1999). Septins: a highly conserved family of membrane-associated GTPases with functions in cell division and beyond. *J. Membr. Biol.* **169**, 75-81.

Vorobjev, I. and Chentsov, Y. (1982). Centrioles in the cell cycle. I. Epithelial cells. *J. Cell Biol.* **98**, 938-949.

Wilson, P. G., Zheng, Y., Oakley, C. E., Oakley, B. R., Borisy, G. G. and Fuller, M. T. (1997). Differential expression of two gamma-tubulin isoforms during gametogenesis and development in Drosophila. *Dev. Biol.* **184**, 207-221.

Yoder, B. K., Hou, X. and Guay-Woodford, L. M. (2002). The polycystic kidney disease proteins, polycystin-1, polycystin-2, polaris, and cystin, are co-localized in renal cilia. *J. Am. Soc. Nephrol.* **13**, 2508-2516.

Zhang, P. and Stankiewicz, R. L. (1998). Y-Linked male sterile mutations induced by P element in Drosophila melanogaster. *Genetics* **150**, 735-744.